Appl Biochem Biotechnol (2014) 172:1517–1529
DOI 10.1007/s12010-013-0642-z

Direct Electron Transfer at a Glucose Oxidase–Chitosan-Modified Vulcan Carbon Paste Electrode for Electrochemical Biosensing of Glucose

Sankararao Mutyala · Jayaraman Mathiyarasu

Received: 14 August 2013 / Accepted: 30 October 2013 /
Published online: 13 November 2013

Abstract This article describes the investigation of direct electron transfer (DET) between *glucose oxidase* (GOD) and the electrode materials in an enzyme-catalyzed reaction for the development of improved bioelectrocatalytic system. The GOD pedestal electrochemical reaction takes place by means of DET in a tailored Vulcan carbon paste electrode surfaces with GOD and chitosan (CS), allowing efficient electron transfer between the electrode and enzyme. The key understanding of the stability, biocatalytic activity, selectivity, and redox properties of these enzyme-based glucose biosensors is studied without using any reagents, and the properties are characterized using electrochemical techniques like cyclic voltammogram, amperometry, and electrochemical impedance spectroscopy. Furthermore, the interaction between the enzyme and the electrode surface is studied using ultraviolet–visible (UV–Vis) and Fourier transform infrared (FTIR) spectroscopy. The present glucose biosensor exhibited better linearity, limit of detection (LOD=0.37±0.02 mol/L) and a Michaelis–Menten constant of 0.40±0.01 mol/L. The proposed enzyme electrode exhibited excellent sensitivity, selectivity, reproducibility, and stability. This provides a simple "reagent-less" approach and efficient platform for the direct electrochemistry of GOD and developing novel bioelectrocatalytic systems.

Keywords Carbon paste electrode · Cyclic voltammetry · Direct electron transfer · Glucose biosensor · Reagent-less · Enzyme electrode

Introduction

Diabetes mellitus is a universal public health problem, and this metabolic chaos is a chronic disease resulting from the deficiency in the insulin emission or insulin action. In this type of patient, glucose in the blood cannot be absorbed by the cells in the body and is reflected by irregular blood glucose concentrations, i.e., higher or lower than the normal range 80–120 mg/dL (0.0044–0.0066 M/L). This disease causes health problem that includes heart

S. Mutyala · J. Mathiyarasu (✉)
Electrodics and Electrocatalysis Division, Central Electrochemical Research Institute (CSIR),
Karaikudi 630 006 Tamilnadu, India
e-mail: al_mathi@yahoo.com

disease, nerve damage, kidney failure, or blindness and finally leads to death and disability. Therefore, monitoring of glucose concentration level is of greater importance because of the huge and rising population of people with diabetes, who require regular and accurate information about their plasma glucose concentrations [1, 2].

Electrochemical biosensors for the determination of glucose plays an important role, since they are suited for this application with enormous advantages like high sensitivity, selectivity, portable size, rapid response time, and low cost. The most commonly used methodology is the application of potentiometric or amperometric enzyme electrodes. In this method, glucose oxidase (GOD) enzyme is attached to the electrode transducers, in which the glucose molecule undergoes electro-oxidation. GOD containing the flavin adenine dinucleotide (FAD) acts as the cofactor accepting electrons in this process, thereby changing to reduced state. Then, the enzyme normally proceeds to their oxidized state by transferring these electrons to molecular oxygen, resulting in the production of hydrogen peroxide. This hydrogen peroxide is measured amperometrically in an appropriate electrode employing suitable redox mediator, resulted in an indirect estimation of glucose which affects the accuracy of the measurement.

On the other hand, the principle of direct electron transfer (DET) allows construction of "reagent-less" electrochemical biosensors [3, 4], but the application has been limited due to a lack of simple approach to immobilize enzyme and the difficulty of achieving DET because a thick insulating protein layer enfolds to the active layer of redox enzyme. So, the task is to develop a matrix for the DET from glucose to active enzyme site, making electron transfer distance as short as possible to design a reagent-less glucose biosensor. To overcome all these difficulties, we have attempted by immobilizing GOD directly on a Vulcan carbon matrix for direct electron transfer. Here, the FAD, a part of GOD molecule, is known to undergo redox reaction where two protons or two electrons are released in the enzyme-catalyzed reaction of glucose. Thus, glucose can be determined in the absence of an external reagent, involving the transfer of electrons directly from GOD to the electrode surface, achieving the concept of reagent-less glucose biosensor.

Very few reports are available on the concept of reagent-less glucose biosensor system [5–8], and some other biomedical devices based on the DET in an enzyme immobilized electrodes [9–14]. Various nanomaterials, such as gold nanoparticles [15, 16], carbon nanotubes [17–19], and graphene [14, 20], have been used to immobilize the enzyme to promote DET of redox enzyme on the surface of electrode. However, for a device fabrication purpose, simple electrode matrix has not been evaluated much in view of a commercial point of view. In the present approach, the direct electron transfer promotion in a simple modified Vulcan carbon paste electrode matrix has been demonstrated. GOD-immobilized Vulcan carbon paste electrode was investigated with an aim to develop reagent-less glucose biosensor. Carbon paste electrode is modified by entrapping the GOD and CS layer by layer using drop-casting method, and the resulted enzyme electrode CS/GOD/carbon paste electrode (CPE) has an intimate contact between enzyme and carbon particles.

Materials and Methods

Materials

The following chemicals were used of analytical grade, and all the solutions were prepared with ultrapure water of 18 MΩ/cm resistivity (Milli-Q, Millipore). Vulcan Carbon XC72R was received from the Cabot Chemical Company, α-D-(+)-glucose anhydrate 96 % was purchased from Sigma-Aldrich, and glucose oxidase (ex, *Aspergillus niger*-lyophilized powder

250,000 U/mg) was received from Sisco Research Laboratory Pvt., Limited, India. Chitosan was obtained from Alfa Aesar, and paraffin oil, disodium hydrogen orthophosphate ($Na_2HPO_4{\cdot}2H_2O$), sodium dihydrogen phosphate ($NaH_2PO_4{\cdot}H_2O$), and acetic acid were received from Merck Company. Potassium ferricyanide and potassium ferrocyanide were received from Ranbaxy Laboratories Limited, India.

Preparation of CPEs

The carbon past electrodes were prepared by mixing 0.006 g of the Vulcan carbon powder with 0.02 mL of paraffin oil on a glass plate followed by homogenization using a glass rod, and this ratio was maintained uniformly for the entire study. The prepared paste was filled into the Teflon tube containing a cavity (outer diameter 3 mm and inner diameter 1.6 mm). A brass rod inserted into the Teflon tube served to establish an electrical contact with the external circuit. The electrode surface was renewed mechanically by smoothing and then polished on a piece of transparent paper followed by careful cleaning with deionized water before performing each electrochemical experiment.

Fabrication of the Enzyme Electrodes

The 0.5 % *w*/*v* chitosan solution was prepared by dissolving 0.5 g of chitosan in 0.2 % *w*/*v* acetic acid with the assistance of sonication, making the final volume to 100 mL with 0.2 % *w*/*v* acetic acid. Sodium dihydrogen phosphate and disodium hydrogen phosphate 2-hydrate were used to prepare phosphate buffer solution (PBS) pH 7.4. Homogeneous dispersion of GOD in a phosphate buffer solution was prepared by dissolving 0.02 g of GOD powder in 1 mL of freshly prepared PBS. These solutions were stored at 4 °C and used throughout the experiments; 0.003 mL of GOD aliquot of the suspension was drop cast on the carbon paste electrode surface. The film was allowed to dry at 4 °C for overnight in phosphate buffer solution, before another aliquot was drop cast. The enzyme-coated electrode was further modified with a thin layer of 0.003 mL chitosan solution and allowed to dry in the dark at 4 °C and referred as CS/GOD/CPE electrode or enzyme electrode. Prior to all measurements, the enzyme electrode was rinsed with PBS to remove the loosely bound protein molecules.

Electrochemical Measurements

All electrochemical measurements were performed using an electrochemical instrument, Palm Sens, Inc., Netherlands. A three-electrode system comprising of an enzyme electrode served as a working electrode, a platinum wire as an auxiliary electrode, and Ag/AgCl as a reference electrode was employed for all electrochemical experiments. All experiments were performed at a room temperature of 25±1 °C in 0.1 M PBS as the supporting electrolyte. Cyclic voltammetric measurements were performed under batch conditions. The cyclic voltammogram was recorded between −0.3 and 0.5 V at a scan rate of 20 mV/s. Amperometric experiments were carried out in a stirred cell with a successive addition of glucose standard solution to the PBS by applying a potential step of 0.3 V to the enzyme electrode. Impedance measurements were performed in an electrochemical cell using Ivium Technologies, Netherlands. Compact-state electrochemical analyzer in 5 mM of potassium ferricyanide + potassium ferrocyanide in 0.1 phosphate buffer solution was used by applying an alternating voltage of 5 mV in a frequency range from 0.01 Hz to 100 kHz, and Thales 4.13 software was used for curve fitting.

Spectroscopic and Microscopic Characterizations

Fourier transform infrared (FTIR) spectra were recorded in the wavelength region of 400–4,000 cm^{-1} with a spectral resolution of 4 cm^{-1} using the Nexus 670 model FTIR spectrometer (Make: Thermo Electron Corporation, USA). The electrode materials were thoroughly ground with high-quality potassium bromide (KBr) made it as pellets and introduced in the IR path. Ultraviolet–visible (UV–Vis) absorption spectra of the electrode biomaterials were collected on the Cary 500 UV–Vis–NIR spectrophotometer in the wavelength range of 200–800 nm. The morphological features with and without enzyme modification of the carbon paste electrodes were investigated using Agilent 5500 atomic force microscopy instrument.

Results and Discussion

UV–Vis Spectroscopy

In general, UV–Vis spectra provide information about the conjugation, unsaturated functional groups, and denaturation of proteins. In the present work, this technique is particularly used to examine the conformational changes in the enzyme electrode in comparison to the bare CPE as shown in Fig. 1. Electronic spectrum of bare Vulcan carbon paste electrode does not show any characteristic absorption peak in the wavelength region of 200–800 nm, whereas the modified enzyme electrode exhibits a distinct absorption peak at 214 and 254 nm, indicating the presence of chromophoric group that causes a conformational change in the molecule when exposed to UV light. This is due to the presence of GOD and amine groups in chitosan on the enzyme electrode surface. The above result confirms that conformational change takes place with finite absorption peaks along with enhanced conjugation.

FTIR Spectroscopy

FTIR characterization was carried out to assess the structural features and functional groups in the electrode materials. Spectrum of Vulcan carbon paste and enzyme electrode is depicted in

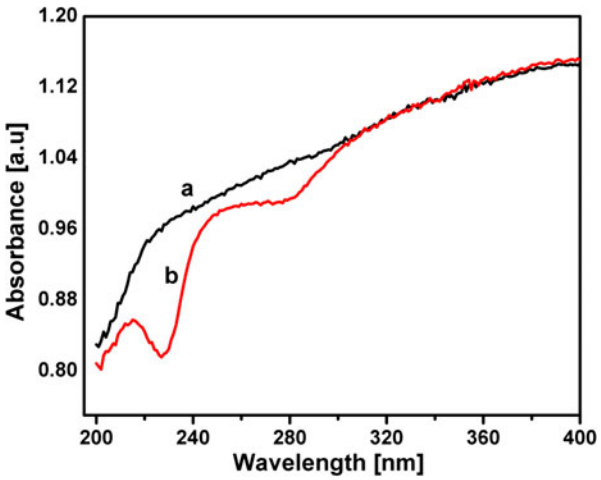

Fig. 1 The UV–Visible spectra of **a** bare Vulcan carbon and **b** enzyme electrode

Fig. 2c, d, and for the sake of comparison, the spectrum of CS and GOD is also presented in Fig. 2a, b. In general, the peaks appeared at more than 2,500 cm^{-1} precisely gives the information about hydrogen bonding in the molecule. In CS and GOD molecule spectrum, the peaks appeared at 3,438 and 3,417 cm^{-1} indicates the –OH stretching frequency. The peaks at 2,921 and 1,424 cm^{-1} denote the –CH symmetric stretching and –NH in-plane bending vibrations of CS molecule, respectively. In addition, the –CO stretches and –OH in-plane bending coupled vibration for different alcoholic groups appeared at 1,373 and 1,047 cm^{-1}. The signals at 1,215 and 1,646 cm^{-1} strongly confirm the free alcoholic and –CO stretching of a tertiary amide bond in CS.

GOD enzyme is having 12 % of carbohydrate (main component is mannose). In GOD spectrum, the prominent peaks appeared at 1,073 and 1,178 cm^{-1} strongly reflect the –C–O–C asymmetric stretching vibration of cyclic ethers in GOD. The –OH in-plane bending vibration peak appeared at 1,240 cm^{-1} along with –CO stretching in enolic form at 1,644 cm^{-1}. In the case of bare Vulcan paste electrode, only very few signals appeared, and among those, the strong peak at 1,628 cm^{-1} indicates the –C=C stretching frequency, and a peak at 673 cm^{-1} is a sign of –CH out-of-plane bending vibrations. The peak appeared at 3,428 cm^{-1} signal corresponds to the –OH stretching vibration. This is due to a fact that a small portion of the carbonaceous materials can easily undergo oxidation with atmospheric oxygen.

Figure 2d shows the spectrum of enzyme electrode, where the peaks emerged at 3,629 and 3,561 cm^{-1} are responsible for alcoholic group, and the signal at 2,996 cm^{-1} reflects to the –CH stretching in cyclic rings. Apart from these, the new peaks appeared at 1,683 and

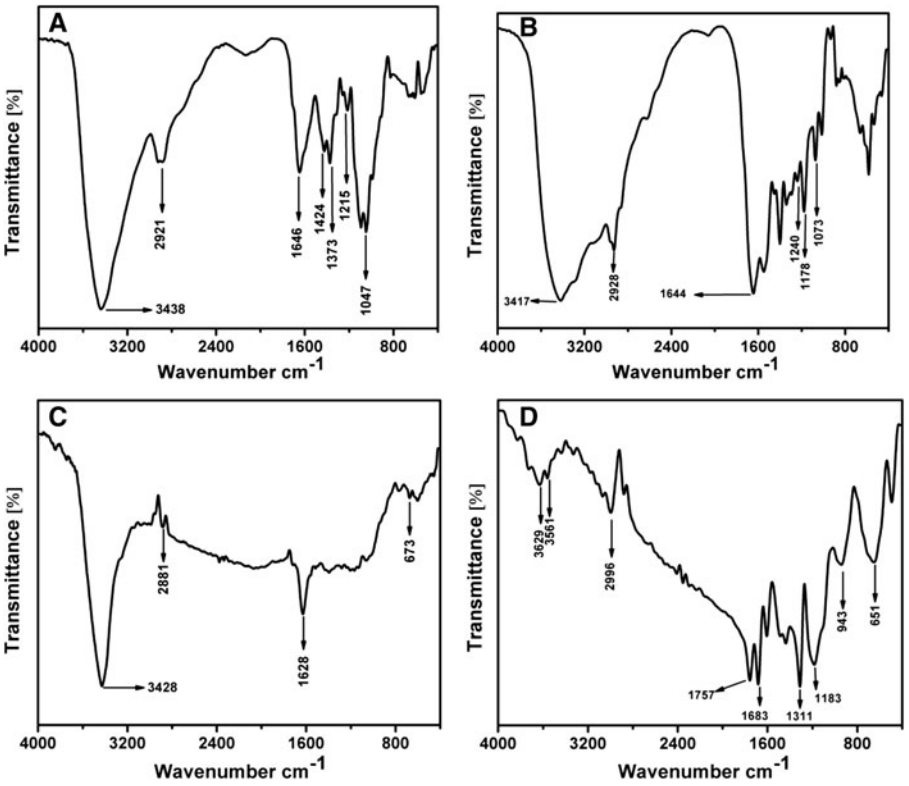

Fig. 2 The FTIR spectrum of **a** chitosan, **b** glucose oxidase, **c** Vulcan carbon, and **d** enzyme electrode, where *T* is a transmittance [*T*=Int/Int (ref)]

1,757 cm^{-1}, corresponding to –CO stretching in GOD and CS. Below the fingerprint region 1,500 cm^{-1}, the peaks appeared at 943 and 651 cm^{-1} are due to the –CH bending vibrations. These results signify that carbon materials have the same hybridization with small structural changes. Further, after modification with biomaterials, the characteristic property of carbon material is retained. However, the newly emerged peaks in the enzyme electrode confirm the presence of GOD and CS, where the enzyme is preserved in its nature after immobilization. Thus, the glucose biosensor configuration has been achieved without using any reagents, and CS–GOD was successfully immobilized on the Vulcan carbon paste electrode with a strong covalent bond formation.

Electrochemical Impedance Spectroscopy Studies

The CPE with and without enzyme immobilization is characterized using the electrochemical impedance spectroscopy (EIS). Figure 3a, b shows the EIS spectrum of bare CPE and enzyme electrodes, respectively. The plot exhibited a typical semicircle behavior while plotting the imaginary number Z'' (w) [where Z'' $(w)=-1/wC$] against real numbers Z' (w), where angular frequency $(w)=2\pi f$ and f is AC frequency. The corresponding equivalent circuit is shown in Fig. 3a. As expected, the charge transfer resistance of enzyme electrode (29.5 KΩ) is higher than the bare CPE (11 KΩ). Increase in impedance clearly indicated the successful immobilization of enzyme and CS on the CPE with a strong adhesion on the electrode surface. Thus, the modification resulted in three times increment in the electrode resistance, and these results have good agreement with the voltammetric and spectral studies.

Cyclic Voltammetry

Figure 4 shows the cyclic voltammogram (CV) of bare CPE and enzyme-modified electrode in 0.1 M PBS (pH 7.4). From the voltammogram, it is observed that CPE does not exhibit redox activity, and it exhibited a usual capacitive behavior in the specified potential region which indicates sluggish heterogeneous electron transfer kinetics. Fascinatingly, a pair of well-defined and nearly symmetric redox peaks was observed with finite peak current at a formal potential of 0.2 V for the enzyme-modified electrode with a calculated peak-to-peak separation (ΔE_p) of 95 mV. Obviously, these peaks were ascribed to the redox behavior of the electroactive site (FAD) of the immobilized GOD with direct electron transfer of the enzyme

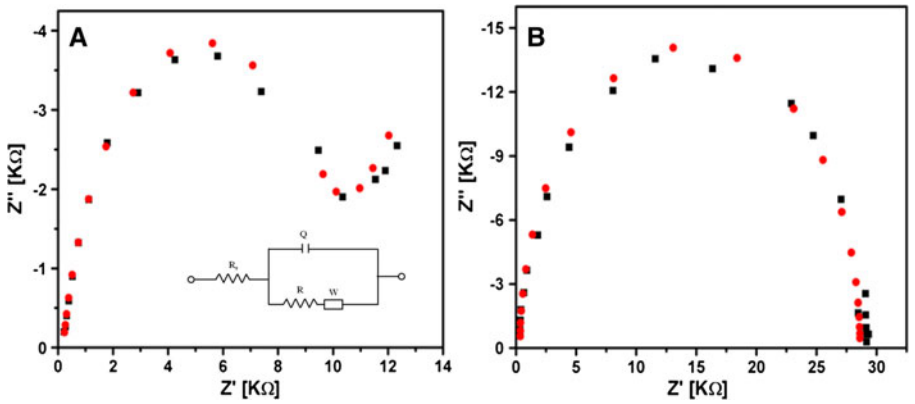

Fig. 3 Electrochemical impedance spectra of **a** bare Vulcan carbon and **b** enzyme electrode, in 5 mM of potassium ferrocyanide + potassium ferricyanide contain 0.1 M PBS (pH 7.4). Corresponding equivalent circuit is given in Fig. 3a. In plots, black dots are original data, and red ones are fitted data

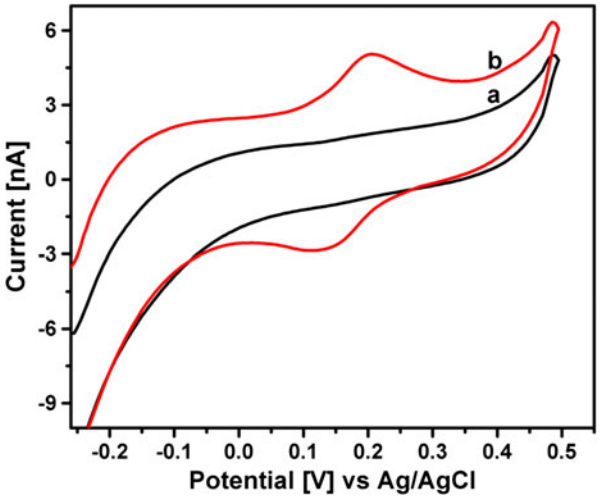

Fig. 4 Cyclic voltammograms of *a* Vulcan carbon paste and *b* enzyme electrode in 0.1 M of PBS pH (7.4) with scan rate 20 mV s^{-1}

with the electrode. Furthermore, the heterogeneous electron transfer constant (K_s) is calculated using the Laviron equation [21]:

$$\log K_s = \alpha\log(1-\alpha) + (1-\alpha)\log\alpha - \log RT/nF\nu - \alpha(1-\alpha)nF\Delta E_p/2.3RT\ldots \quad (1)$$

where n is the number of electrons transferred that involved in the electrode reaction (n=2); F is the Faraday constant, coulombs per mole; K_s is the heterogeneous electron transfer rate constant, per second; ν is the scan rate, volts per second; R is the gas constant, joules per kilogram per mole; T is the absolute temperature, kelvins; and α is the transfer coefficient (α=0.5).

The results showed that bare CPE does not show significant K_s value, whereas enzyme electrode surface showed a value of 1.6×10^{-2} s^{-1}. The exchange current density of bare CPE and enzyme electrode is found to be 250 and 337 μA/cm^2, respectively. This revealed that the prepared enzyme electrode exhibited a finite K_s value with increased exchange current density, and definite amount of electroactive enzyme is successfully bonded on the Vulcan carbon paste electrode. In addition, GOD enzyme electrode has enhanced electroactive surface area compared with the bare CPE. However, the redox activities of the enzyme molecules are always difficult to observe at the common electrode materials such as glassy carbon or graphitic electrodes. This is because of the enzyme molecule having a homodimer containing two tightly bound FAD, which is deeply buried in the protein structure and not easily accessible for direct electron transfer reaction at the electrode surface. Herein, the Vulcan carbon showed its robust ability for the direct electron transfer from the enzyme cavity to the electrode surface.

$$\mathrm{GOD/FAD} + 2e^- + 2H^+ \rightarrow \mathrm{GOD/FADH_2}. \quad (2)$$

Furthermore, the enzyme-immobilized CPE is characterized by atomic force microscopy. Figure 5 shows the morphology of CPE with and without enzyme immobilized on the surface. The bare carbon paste electrode showed a porous morphology which is the characteristic of a typical carbon paste electrode. However, the enzyme-immobilized electrode showed the aggregates of the trapped biomolecules on its surface. Thus, the porous carbon structure facilitated immobilization of the enzyme to expose the enzymatic activity sites and made the substrate more easily accessible to the enzyme, resulting in a good amperometric response of the biosensor.

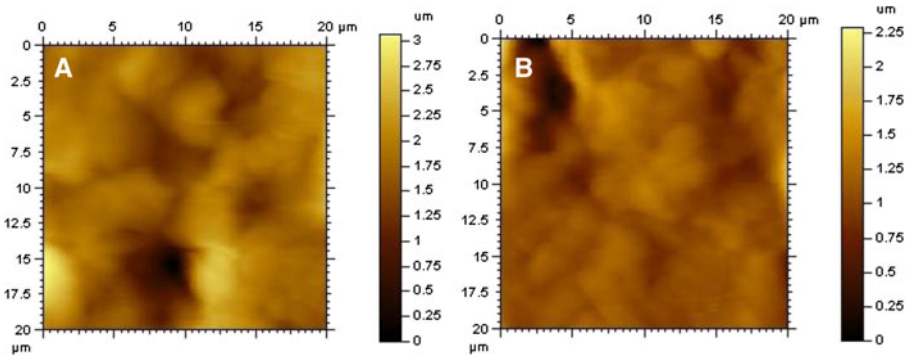

Fig. 5 Atomic force micrographs of the CPE immobilized with enzyme (**a**) and without enzyme (**b**)

Effect of scan rate on the electrochemical performance of GOD enzyme-immobilized Vulcan carbon paste electrode is shown in Fig. 6. From the figure, it is observed that the anodic and cathodic peak current increased with the scan rate. The anodic and cathodic peak potential values of enzyme electrode showed a potential shift in the respective directions. The potential difference (ΔE_p) was ranged from 95 mV at a scan rate of 20 mV s^{-1} to 125 mV at 100 mV s^{-1}, indicating that the Randles–Sevcik behavior, which is attributed to enzyme electrode, has a surface-confined electrochemical redox process [22].

$$i_p = 2.69 \times 10^5 n^{3/2} A C D^{1/2} \nu^{1/2} \tag{3}$$

where i_p is the peak current, amperes; n is the number of electrons transferred in the redox event; A is the electrode area, square centimeters; F is the Faraday constant, coulombs per mole; D is the diffusion coefficient, square centimeters per second; C is the concentration, mole per cubic centimeter; and ν is the scan rate, volts per second.

The relationship between the cathodic and anodic peak currents over a range of scan rate for the enzyme electrode is shown in Fig. 7. It shows a linear dependence with scan rate, and the

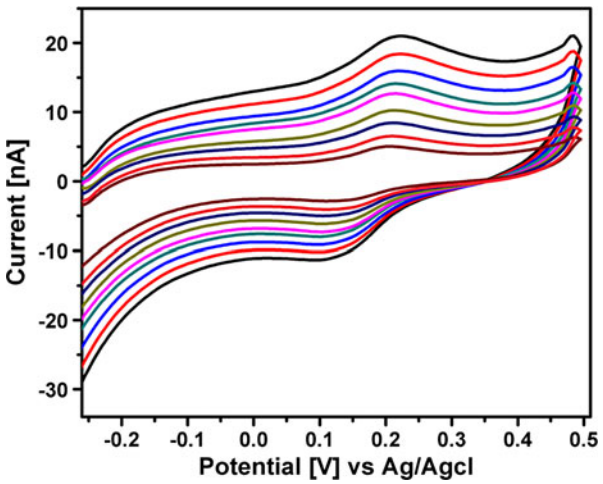

Fig. 6 Cyclic voltammograms of enzyme electrode recorded in 0.1 M PBS at different scan rates. The scan rates from inner to outer are 20, 30, 40, 50, 60, 70, 80, 90, and 100 mV s^{-1}

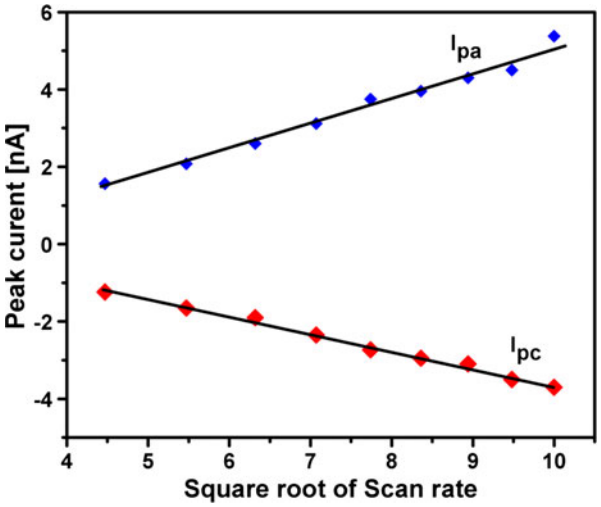

Fig. 7 The linear dependence of I_{pa} (*upper*) and I_{pc} (*lower*) on scan rate (20–100 mV s^{-1})

correlation coefficient (R^2) values for anodic peak current (i_{pa}) and cathodic peak current (i_{pc}) are 0.98 and 0.99, respectively.

Performance of the CS/GOD/CPE in the Presence of Glucose

Figure 8 depicts the specific activity of GOD in the fabricated enzyme electrode in 0.1 M PBS electrolyte in the absence and presence of 5 mM of glucose. Interestingly, addition of glucose enhances the oxidation peak current drastically, which confirm the catalytic reaction occurring between GOD and glucose, as portrayed in Scheme 1. This further entails that the immobilized GOD possesses high enzymatic activity, and CS/GOD/CPE electrode provides a suitable

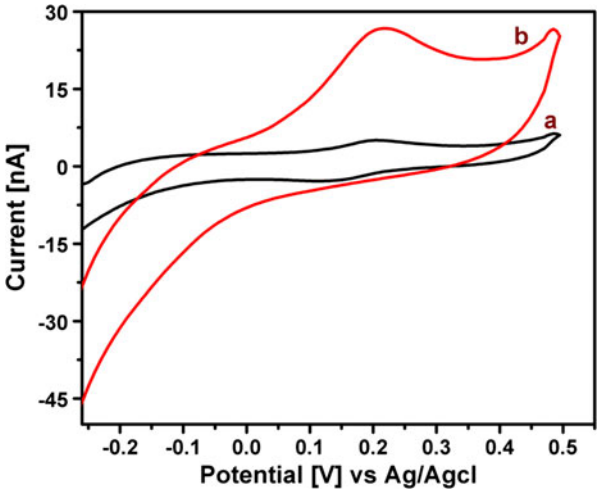

Fig. 8 Cyclic voltammograms of enzyme electrode in 0.1 M PBS in the absence (*a*) and in the presence of 5 mM glucose (*b*). Scan rate is 20 mV s^{-1}

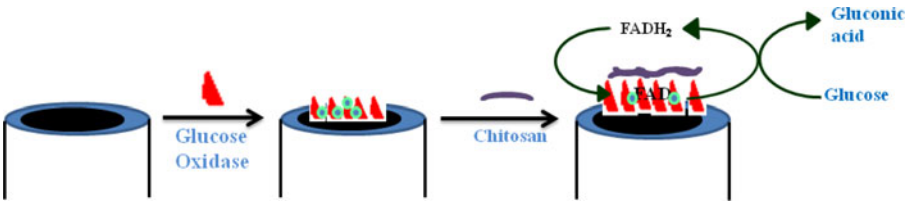

Scheme 1 Schematic representation of DET reaction mechanism on the enzyme electrode

environment for GOD to perform DET at enzyme-modified electrodes. The activity of enzyme electrode shows a specific response to glucose, and it is further verified with amperometric experiments.

Amperometric Determination of Glucose with Enzyme Electrode

Figure 9 shows the amperometric response of the glucose biosensor using enzyme electrode. The measurements were carried out in a PBS (0.1 M) of pH 7.4 as a supporting electrolyte. Amperometric batch measurements were conducted under forced convection (stirring) mode by applying a constant potential of 0.3 V. Figure 10 exhibited the amperometric current response of the successively added 5 mM glucose, where the reaction takes place between the oxidized forms of GOD and glucose. During this process, the electrons are released, thereby transforming the chemical signal, which is proportional to the glucose concentration [23]. Thus, reagent-less glucose biosensor using an enzyme electrode is achieved, which encompass high sensitivity and selectivity in a range of glucose concentrations with an enhanced current response in a stepwise addition of glucose. Few reports describing the amperometric enzyme based glucose biosensors employing the concept of mediator-less electrodes, where a direct communication between the active site of the enzyme and the electrode results in significant current density in the presence of enzyme substrates [14]. In some cases, the improved behavior of enzyme electrode could be accounted with the metal

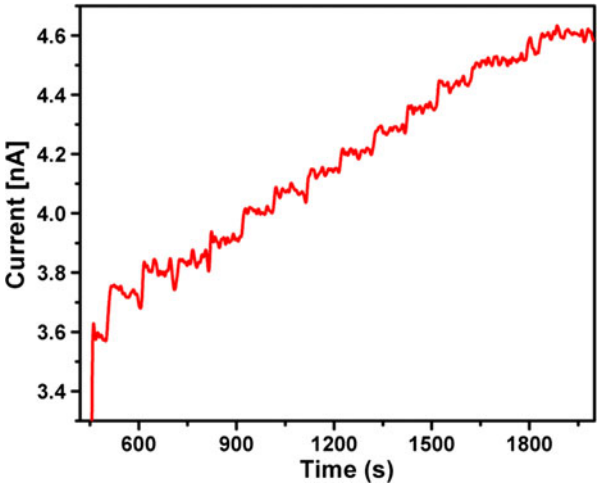

Fig. 9 The amperometric response of 5 mM addition of glucose using an enzyme electrode in 0.1 M PBS (pH 7.4) supporting electrolyte

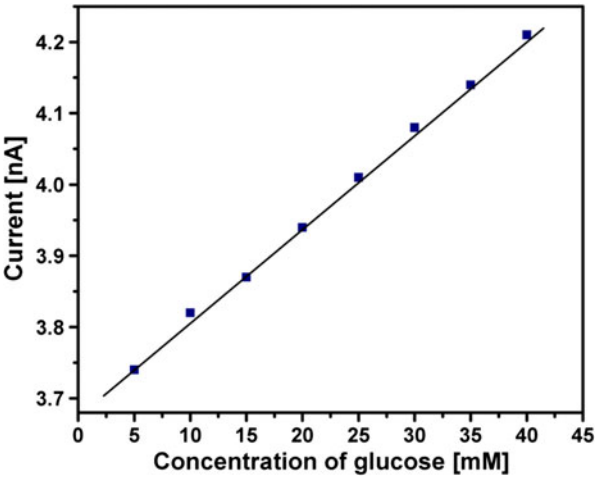

Fig. 10 Calibration graph of the amperometry response of peak current versus glucose concentration

impurities present in the Vulcan carbon that plays a key role in such extraordinary catalytic performance [24]. This is established by many researchers on various carbon materials exploited for sensor and electrocatalytic applications [25–30]. Thus, the typical reagent-less enzyme electrode give large signals with a linear response as shown in Fig. 10, and the correlation coefficient value (R^2) is found to be 0.99 for enzyme electrode with a LOD of 0.37 ±0.02 mol/L. The sensitivity of the fabricated electrode is found to be 0.013 nA mM^{-1} for a linear concentration range of 1 to 40 mM of glucose, and the response time of the enzyme electrode is calculated as 10 s. The apparent Michaelis–Menten constant (K_m) is calculated as 0.40±0.01 mol/L obtained from the Lineweaver–Burk equation that confirms that the enzyme electrode shows an outstanding electrocatalytic activity. The comparison of previous reported work on direct glucose sensing and the present work is given in Table 1.

Table 1 Comparison of different modified electrodes for the direct glucose estimation

Modified electrode	Linearity (mM)	Sensitivity (nA mM^{-1} cm^{-2})	K_m^{app} (M)	Detection limit (M)	Reference
CMM	7.9	58.8	0.0044	0.010	[31]
Pt–CMM	4.2	1.0	0.0034	0.001	[32]
GOx–$NdPO_4$ NPs–CS–GCE	10	1,920	–	–	[33]
Pt–CMK_3–GOD–gelatin–GCE	12.2	–	0.01	0.001	[34]
GOD–GMWCNT–GCE	20.09	2,470	–	–	[35]
GOD–Au–CPE	0.28	840	–	1×10^{-4}	[7]
GOD–graphene–CS–GCE	12.0	3,793	–	2×10^{-5}	[14]
GOD–CNT–GCE	1	2,000	–	2×10^{-4}	[5]
Graphene–AuNPs–GOD–CS–Au electrode	10	550	–	18×10^{-5}	[20]
Graphene–GOD–PFIL–GCE	14	–	–	–	[22]
CS–GOD–CPE	5	0.013	0.40	0.37	Present work

Conclusions

In this work, we report a simple fabrication of enzyme electrode for glucose estimation which involves the newer concept of reagent-less glucose biosensor. This is based on the immobilization of highly sensitive GOD and CS biomaterials on Vulcan carbon matrix, and this matrix is fabricated in the form of conventional carbon paste electrode. The direct electrochemistry of immobilized GOD revealed that the Vulcan carbon-based biomatrices greatly improved the DET of FAD active group in the glucose oxidase enzyme with the carbon electrode surface resulted in a precise and finite reversible redox peaks. The resulting biosensor is capable of detecting glucose of 0.005 mol/L level and may be useful for real sample analysis since it has exhibited excellent operational stability and selectivity. This study clearly indicates that it is a simple methodology for the immobilization of GOD in a sensor matrix and also provides a model technique for the potential application of reagent-less glucose sensors for the development of bioelectrocatalytic systems.

Acknowledgments The authors gratefully acknowledge the financial support DST/TSG/PT/2009/82 from the Department of Science and Technology, New Delhi.

References

1. The Diabetes Control and Complications Trial (DCCT) Research Group. (1993). *The New England Journal of Medicine, 329*, 977–986.
2. Sieg, A., Guy, R. H., & Begona Deldago-Charro, M. (2004). *Journal of Pharmaceutical Sciences, 50*, 1383–1390.
3. Sekretaryova, A. N., Vokhmyanina, D. V., Chulanova, T. O., Karyakina, E. E., & Karyakin, A. A. (2012). *Analytical Chemistry, 84*, 1220–1223.
4. Dai, Z., Yan, F., Chen, J., & Ju, H. (2003). *Analytical Chemistry, 75*, 5429–5434.
5. Luo, X., Killard, A. J., & Smyth, M. R. (2006). *Electroanalysis, 18*, 1131–1134.
6. Gortan, L., Karan, H. I., Hale, P. D., Inagaki, T., Okamoto, Y., & Skothim, T. A. (1990). *Analytica Chimica Acta, 228*, 23–30.
7. Liu, S., & Ju, H. (2003). *Biosensors and Bioelectronics, 19*, 177–183.
8. Rivas, G. A., Rubianes, M. D., Pedano, M. L., Ferreyra, N. F., Luque, G. L., Rodrguez, M. C., et al. (2007). *Electroanalysis, 19*, 823–831.
9. Wu, S., Ju, X. H., & Liu, Y. (2007). *Advanced Functional Materials, 17*, 585–592.
10. Liu, K. P., Zhang, J. J., Yang, G. H., Wang, C. M., & Zhu, J. J. (2010). *Electrochemistry Communications, 12*, 402–405.
11. Xiao, C. H., Chu, X. C., Wu, B. H., Pang, H. L., Zhang, X. H., & Chen, J. H. (2010). *Talanta, 80*, 1719–1724.
12. Nadzhafova, O., Etienne, M., & Walcarius, A. (2007). *Electrochemistry Communications, 9*, 1189–1195.
13. Wu, H., Wang, J., Kang, X. H., Wang, C. M., Wang, D. H., Liu, J., et al. (2009). *Talanta, 80*, 403–406.
14. Kang, X. H., Wang, J., Wu, H., Aksay, I. A., Liu, J., & Lin, Y. H. (2009). *Biosensors and Bioelectronics, 25*, 901–905.
15. Jia, F., Shan, C. S., Li, F. H., & Niu, L. (2008). *Biosensors and Bioelectronics, 24*, 945–950.
16. Pingarron, J. M., Yanez-Sedeno, P., & Gonzalez-Cortes, A. (2008). *Electrochimica Acta, 53*, 5848–5866.
17. Azamian, B. R., Davis, J. J., Coleman, K. S., Bagshaw, C. B., & Green, M. L. H. (2002). *Journal of American Chemical Society, 124*, 12664–12665.
18. Wen, D., Liu, Y., Yang, G. C., & Dong, S. J. (2007). *Electrochimica Acta, 52*, 5312–5317.
19. Joseph, W., & Mustafa, M. (2003). *Analytical Chemistry, 75*, 2075–2079.
20. Shan, C. S., Yang, H. F., Han, D. X., Zhang, Q., Ivaska, A., & Niu, L. (2010). *Biosensors and Bioelectronics, 25*, 1070–1074.

21. Laviron, E. (1979). *Journal of Electroanalytical Chemistry, 101*, 19–28.
22. Shan, C. S., Yang, H. F., Song, J. F., Han, D. X., Ivaska, A., & Niu, L. (2009). *Analytical Chemistry, 81*, 2378–2382.
23. Portaccio, M., Durante, D., & Viggiano, A. (2007). *Electroanalysis, 19*, 1787–1793.
24. Sankararao, M., Anandhakumar, S., & Mathiyarasu, J. (2013). SWOT the electrochemical reactivity of different carbon paste electrodes. Unpublished work.
25. Chng, E. L. K., & Pumera, M. (2011). *Chemistry of Asian Journal, 6*, 2304–2307.
26. Wang, J., Pamidi, P. V. A., Renschler, C. L., & White, C. (1996). *Journal of Electroanalytical Chemistry, 404*, 137–142.
27. Guiseppi-Elie, A., Lei, C. H., & Baughman, R. H. (2002). *Nanotechnology, 13*, 559–564.
28. Cai, C. X., & Chen, J. (2004). *Analytical Biochemistry, 332*, 75–83.
29. Ambrosi, A., & Pumera, M. (2011). *Journal of Physical Chemistry C, 115*, 25281–25284.
30. Pumera, M., Ambrosi, A., & Khim Chng, E. L. (2012). *Chemical Science, 3*, 3347–3355.
31. You, C. P., Xu, X., Tian, B. Z., Kong, J. L., Zhao, D. Y., & Liu, B. H. (2009). *Talanta, 78*, 705–710.
32. You, C. P., Li, X., Zhang, S., Kong, J. L., Zhao, D. Y., & Liu, B. H. (2009). *Microchimica Acta, 167*, 109–116.
33. You, C. P., Li, X., Zhang, S., Kong, J. L., Zhao, D. Y., & Liu, B. H. (2009). *Bioelectrochemistry, 74*, 246–253.
34. Yu, J., Yu, D., Zhao, T., & Zeng, B. (2008). *Talanta, 74*, 1586–1591.
35. Periasamy, A. P., Chang, Y. J., & Chen, S. M. (2011). *Bioelectrochemistry, 80*, 114–120.